Supplementary Material of "Dominant-Eye-Aware Asymmetric Foveated Rendering for Virtual Reality"

Zhimin Wang, Xiangyuan Gu, and Feng Lu, *Senior Member, IEEE*

A. Explanation of Hypotheses

Our hypotheses are:

H_1: *For a given eye (e.g., the dominant eye), the foveation parameter σ_1 for the inner layer remains constant at maximum rendering speedup, regardless of e_1 value.*

Our hypothesis suggests that the foveation level of the inner layer is determined by the eye's perception of the central visual field. Since central vision is the most sensitive, it establishes the limit for foveation parameter σ_1. Consequently, we argue that variations in e_1 do not influence the perception of the central visual field.

H_2: *For a given eye (e.g., the dominant eye), if e_1 is fixed, the foveation parameter σ_2 for the middle layer remains constant at maximum rendering speedup for any e_2 value.*

For instance, let e_1 and e_2 have values of $\{10°, 20°\}$ and $\{10°, 30°\}$, respectively. We assume that the value of σ_2 remains constant when achieving the maximum rendering speedup. The reason is similar to H_1 that the eye is more sensitive to areas near the fixation point compared to peripheral regions. Consequently, the area in $[e_1, e_2]$ near the boundary e_1 determines the upper limit of the foveation parameter σ_2. Therefore, regardless of how much e_2 is enlarged or reduced, it will not affect the perception of the middle layer.

B. Main Test

The objective of this study is to determine an optimal set of parameters that maximizes rendering acceleration while preserving perceptual quality. Participants first identify their dominant eye using the Miles Test. In the Main Test, participants keep both eyes open and the visual content for both eyes is rendered simultaneously. Measurements of eccentricity and the σ parameter are conducted sequentially, beginning with the dominant eye and followed by the non-dominant eye.

Participants are provided with a brief introduction to the experiment, followed by a warm-up trial to help them familiarize themselves with the tasks. The Main Test lasts approximately 50 minutes. To prevent visual fatigue, participants are instructed to close their eyes and rest briefly between each step.

Zhimin Wang, Xiangyuan Gu, and Feng Lu are with the State Key Laboratory of Virtual Reality Technology and Systems, School of Computer Science and Engineering, Beihang University, Beijing 100191, China. e-mail: {*zm.wang* \ *guxy* \ *lufeng*}@buaa.edu.cn.

Feng Lu is the corresponding author.

Manuscript received January 10, 2025.

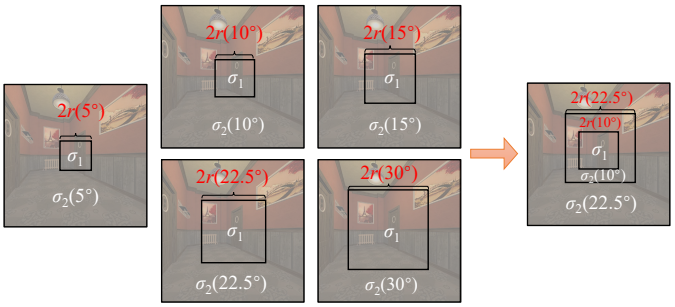

Fig. 1: The measurement process for foveation parameters in two-nested layer images and the construction process for three-nested layer images (this figure is identical to Figure 7 in the main paper).

TABLE I: The bisection intervals to measure the σ of the dominant eye.

Adjusted σ	e_1	Interval
$\sigma_2^d(5)$	10	$[\sigma_1^d, 6.0]$
$\sigma_2^d(10)$	20	$[\sigma_2^d(5), 6.0]$
$\sigma_2^d(15)$	30	$[\sigma_2^d(10), 6.0]$
$\sigma_2^d(22.5)$	45	$[\sigma_2^d(15), 6.0]$
$\sigma_2^d(30)$	60	$[\sigma_2^d(22.5), 6.0]$

Method for Measuring σ: The measurement of the σ parameter is conducted using a binary search method. The interval $[l, r]$ is initially defined, and the midpoint $m = (l+r)/2$ is applied as the foveation level for the test image. The goal is to find the highest level of foveation that is perceptually equivalent to the reference with full-resolution rendering. Participants use a 5-point Likert scale to rate their perceived difference between the two images (5: indistinguishable; 1: highly distinguishable). We iteratively search the σ as follows:

- If the score $s \geq 4$, the difference is deemed acceptable, and σ was refined to the interval $[m, r]$.
- Otherwise, the difference was considered unacceptable, and σ was refined to the interval $[l, m]$.

This process is repeated until the interval width is less than a predefined threshold ε, yielding the measured σ.

The visual content of each eye is a two-nested layer image, as shown in the left of Fig. 1. We record the area whose eccentricity is less the e_1 as the inner region. Otherwise record

TABLE II: Rendering time and frame rates (in FPS) comparison on **UE4 Sun Temple**. Evaluated on full-resolution rendering, 2R (DEAMP), 6R (DEAMP), and DEA-FoR (Ours) on binocular screens (1600×1600 per eye).

Procedure (ms)	Full-resolution	2R (DEAMP)		6R (DEAMP)		DEA-FoR (Ours)	
		dom	n-dom	dom	n-dom	dom	n-dom
Depth Pass	0.14	0.13	0.13	0.13	0.13	0.13	0.13
Shadow Pass	0.16	0.13	0.13	0.13	0.13	0.13	0.13
Defer Pass	5.73	4.34	4.35	4.32	4.33	4.35	4.38
Skybox	0.01	0.01	0.01	0.00	0.00	0.00	0.00
Shading/Pass1	24.52	3.23	2.96	3.05	2.63	**2.50**	**2.39**
Pass2	/	0.06	0.05	0.05	0.06	0.05	0.06
TAA	0.29	0.23	0.23	0.23	0.23	0.23	0.23
Total	30.85	8.13	7.86	7.91	7.5	**7.39**	**7.32**
Binocular Time (ms)	61.70	15.99		15.41		**14.71**	
Fps	16.2	62.5		64.9		**68.0**	

as the outer region.

- **Inner Region of the Dominant Eye**: The value of σ_1^d was determined with an initial binary search interval $[1.0, 4.0]$, with the same σ applied to both eyes during measurement.
- **Outer Region of the Dominant Eye**: The boundary eccentricity e_1 of the inner layer is varied through the set $\{5°, 10°, 15°, 22.5°, 30°\}$. The σ value for the inner layer is fixed to the previously measured σ_1^d, and σ_2 for the outer layer was determined through binary search. The intervals were defined in Table I.

The experiment utilizes the two-nested layer structures to measure one σ_1 and five σ_2 values for the dominant eye, as shown in Fig. 1. Using these measured σ parameters, three-nested layer images are constructed. After completing all measurements for the dominant eye, according to the Equation (11), we calculate the maximum speedup S_d for each image, along with its corresponding eccentricity values (e_1^d, e_2^d).

Next, the parameters for the non-dominant eye are measured using a similar procedure. During this process, the dominant eye's parameters are fixed to the previously measured maximum acceptable values. Similarly, the speedup S_n and the optimal eccentricity values (e_1^n, e_2^n) for the non-dominant eye are determined.

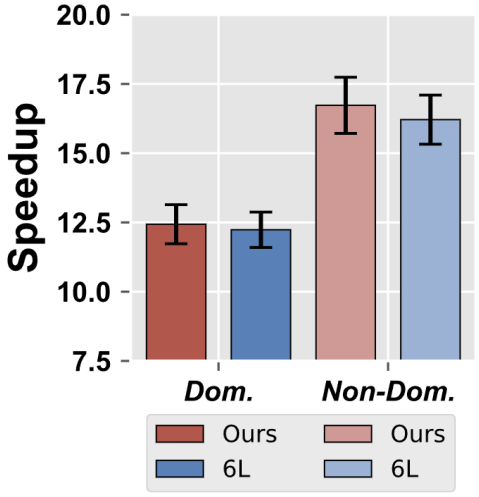

Fig. 2: The comparison of our data collection method with the 6L collection method in [1] about the maximum speedup results for the dominant and non-dominant eyes. The results show no statistically significant differences between the two methods.

C. Validation test results

We conducted a validation test to assess the rationality of our data collection method. The results are presented in Fig. 2. They indicate no significant differences in speedup between the two methods (dominant eye: $t_{21} = 0.546, p = 0.591$; non-dominant eye: $t_{21} = 1.031, p = 0.314$). This confirms that our approach of constructing three-nested layers using two-nested layers is equivalent to directly measuring three-nested layers.

D. Scene Complexity Measurement and Automated Parameter Selection

This paper distinguished between complex and simple scenes based on subjective perception. Below, we discuss our conceptual framework for measuring scene complexity.

Scene complexity can be measured through texture spatial frequency and geometric complexity. Regarding texture spatial frequency, high-frequency textures (such as the wooden planks in scene (a)) contain abundant detail, whereas low-frequency textures (such as the walls in scene (b) and the road in scene (c)) are visually simple. Texture complexity can be quantified by analyzing gradient variations within textures. Regarding geometric complexity, scene (c) contains numerous straight lines and regular geometric shapes and is therefore considered to have low complexity. In contrast, the potted plants in scene (a) exhibit numerous curves and irregular shapes, resulting in high complexity. Geometric complexity can be quantified by analyzing polygon density. Therefore, scene complexity can be quantified by computing both texture spatial frequency and geometric complexity metrics.

Regarding optimal parameter selection, we propose an automatic selection scheme. For example, concerning the selection of foveation parameters for the outermost periphery of the visual field, we establish correlations between the aforementioned scene complexity quantification metrics and foveation parameters through neural networks. By training correspond-

ing models using collected data, the system can directly output foveation parameters based on scene complexity during the testing phase. Other DEA-FoR parameters can be determined through similar approaches.

E. Additional Rendering Time Evaluation

The data shown in Table II of the main paper was collected from a single scene (Rendering Resources [2]) under fixed camera orientation and lighting conditions. Each timing value represents the average over multiple consecutive frames to reduce runtime fluctuation and ensure stability.

We also recognize that the performance results presented in Table II of the main paper may vary across different scenes and viewpoints. Therefore, we conduct an additional evaluation using a more complex scene (the Sun Temple scene from Unreal Engine [3]) under the same experimental conditions. The results from this scene show similar trends. Our DEA-FoR method achieves a 4.19× speedup, compared to DEAMP [1] which achieves a 4.0× speedup, thereby supporting our conclusions. The updated comparison is included in the Table II of this document.

REFERENCES

[1] Z. Wang, X. Gu, and F. Lu, "Deamp: Dominant-eye-aware foveated rendering with multi-parameter optimization," in *2023 IEEE International Symposium on Mixed and Augmented Reality (ISMAR)*. IEEE, 2023, pp. 632–641.

[2] B. Bitterli, "Rendering resources," 2016, accessed: 2025-06-03. [Online]. Available: https://benedikt-bitterli.me/resources/

[3] E. Games, "Unreal engine sun temple, open research content archive (orca)," October 2017, accessed: 2025-06-03. [Online]. Available: https://developer.nvidia.com/ue4-sun-temple